A&A 412, 597–601 (2003)
DOI: 10.1051/0004-6361:20031362

Astronomy & Astrophysics

Dielectronic recombination data for dynamic finite-density plasmas

III. The beryllium isoelectronic sequence

J. Colgan[1], M. S. Pindzola[1], A. D. Whiteford[2], and N. R. Badnell[2]

[1] Department of Physics, Auburn University, Auburn, AL 36849, USA
[2] Department of Physics, University of Strathclyde, Glasgow G4 0NG, UK

Received 20 May 2003 / Accepted 13 August 2003

Abstract. Dielectronic recombination data for the beryllium isoelectronic sequence has been calculated as part of the assembly of a dielectronic recombination database necessary for modelling of dynamic finite-density plasmas (Badnell et al. 2003, A&A, 406, 1151). Dielectronic recombination coefficients for a selection of ions from this sequence are presented and the results discussed.

Key words. atomic data – atomic processes – plasmas

1. Introduction

The programme to generate a total and final state level-resolved intermediate coupling dielectronic recombination database necessary for spectroscopic modelling of dynamic finite-density plasmas, where the coronal approximation is not valid, has been described by Badnell et al. (2003). To this end, work has been underway in calculations of dielectronic recombination data for the oxygen (Zatsarinny et al. 2003) isoelectronic sequence. In this paper we describe calculations and results for dielectronic recombination data for the beryllium isoelectronic sequence. Although some studies of this sequence have been made, most of these present only total recombination rates from the ground state. Here we present final-state level-resolved recombination rates from metastable states as well as the ground state.

There have already been some studies of dielectronic recombination for many of the ions in the beryllium isoelectronic sequence. Badnell (1987) calculated dielectronic recombination rate coefficients in both *LS* and intermediate-coupling schemes for sixteen beryllium-like ions. It was found that both $\Delta n = 0$ and $\Delta n \neq 0$ transitions were important in these calculations, and also that radiative stabilisation of the spectator electron can contribute significantly to dielectronic recombination. The first measurements of dielectronic recombination rate coefficients were subsequently made by Dittner et al. (1987), for the $2s \rightarrow 2p$ excitation in the light ions C^{2+}, N^{3+}, O^{4+} and F^{5+}. Here the fractions of ions in the metastable states of the term $2s2p^3P$ were measured allowing precise comparison with theoretical calculations. However it was clear that (unknown) external electric fields in the interaction region had a significant effect on the magnitude of the dielectronic recombination rate coefficients.

Chen & Crasemann (1988) used a relativistic Dirac-Fock model to study dielectronic recombination in the heavier beryllium-like ions Zn^{26+}, Se^{30+}, Kr^{32+}, Mo^{38+}, Ag^{43+}, and Xe^{50+}, using intermediate-coupling with configuration interaction. This work provided quite accurate dielectronic recombination rate coefficients for both $\Delta n = 0$ and $\Delta n \neq 0$ transitions. Badnell & Pindzola (1989), in their study of intermediate-coupling effects on dielectronic recombination in oxygen ions, presented improved theoretical calculations for O^{4+} ions. A partitioned configuration-average approximation was employed to take into account field effects which showed good agreement with the measurements of Dittner et al. (1987).

New experimental measurements, using merged-beams techniques, were made for some beryllium-like ions at the University of Aarhus. These were compared with theoretical calculations (Badnell et al. 1991) made using the AUTOSTRUCTURE package. The increased precision of the experiment allowed resolution of dielectronic recombination from both the ground and metastable states, results with which the theoretical calculations were in good agreement. Again, the external field enhancement of dielectronic recombination in the measurements did not allow a quantitative comparison between theory and experiment. Other intermediate-coupling calculations of dielectronic recombination rate coefficients for B^+ were made by Pindzola & Badnell (1992). The calculations of

Send offprint requests to: J. Colgan, e-mail: jcolgan@lanl.gov

Badnell (1987), Badnell & Pindzola (1989), and Pindzola & Badnell (1992) have been fitted by Mazzotta et al. (1998) in their study of ionization balance for a wide range of atomic ions.

The current work presents intermediate-coupling calculations of dielectronic recombination final state level-resolved rate coefficients for all ions in the beryllium-like isoelectronic sequence up to Ar^{14+} as well as Ca^{16+}, Ti^{18+}, Cr^{20+}, Fe^{22+}, Ni^{24+}, Zn^{26+}, Kr^{32+}, Mo^{38+}, and Xe^{50+}. As previously discussed (Badnell et al. 2003) this data will form part of an Atomic Data and Analysis Structure (ADAS) dataset comprising the *adf09* files for each ion, detailing the rate coefficients to each *LS* and *LS J*-resolved final state. This is available though the ADAS project (Summers 2001) and is also available online at the Oak Ridge Controlled Fusion Atomic Data Center.

These calculations produce dielectronic recombination final state level-resolved coefficients over a wide range of electron temperatures and atomic ions. No electric or magnetic field effects that may effect dielectronic recombination rates in a plasma are included in these calculations. However we expect our results to be broadly accurate over a wide range, especially our intermediate-coupling calculations. *LS*-coupling calculations are also presented for comparison. In Sect. 2 we give a brief description of the theory used and in Sect. 3 we present some dielectronic recombination rate coefficients for selected ions in the beryllium isoelectronic sequence. We conclude with a brief summary.

2. Theory

The theoretical details of our calculations have already been described in detail (Badnell et al. 2003). Here we outline only the main points. The AUTOSTRUCTURE code (Badnell 1986, 1997; Badnell & Pindzola 1989) is used to calculate energy levels, radiative, and autoionization rates in the *LS* and intermediate-coupling approximations. The autoionization rates are calculated in the isolated resonance approximation using distorted waves. The enables the generation of final state level-resolved and total dielectronic recombination rate coefficients in the independent processes approximation, i.e. we neglect interference between the radiative recombination and the dielectronic recombination rate. Although this has been found to be only a very small effect for the total rate (Pindzola et al. 1992), more recent studies of partial recombination cross sections for lithium-like F^{6+} (Mitnik et al. 1999) predict some interference between these processes for the weak partial cross sections.

The dielectronic recombination process for beryllium-like ions can be represented, in intermediate coupling, for $\Delta n = 0$ excitation, by

$$\begin{aligned} 1s^2 2s^2[^1S_0] + e^- &\rightarrow 1s^2 2s2p[^3P_{2,1,0}\ ;\ ^1P_1]nl, \\ &\searrow\ 1s^2 2p^2[^1S_0\ ;\ ^3P_{2,1,0}\ ;\ ^1D_2]nl, \end{aligned} \quad (1)$$

and

$$\begin{aligned} 1s^2 2s2p[^3P_{2,1,0}] + e^- &\rightarrow 1s^2 2s2p[^3P_{2,1,0}\ ;\ ^1P_1]nl, \\ &\searrow\ 1s^2 2p^2[^1S_0\ ;\ ^3P_{2,1,0}\ ;\ ^1D_2]nl \end{aligned} \quad (2)$$

which can radiatively decay emitting a photon when either the 2p electron drops into the 2s subshell or when the *nl* electron drops into a lower nl' shell which is bound. In this case l and n values were included up to 15 and a quantum-defect approximation for high-level values of n up to 1000 was used (Badnell et al. 2003). For $\Delta n = 1$ excitation the dielectronic recombination process can be written as

$$\begin{aligned} &1s^2 2s^2[^1S_0] + e^- \rightarrow 1s^2 2l3l'[^{3,1}L_J]nl'' \\ &1s^2 2s2p[^3P_{2,1,0}] + e^- \rightarrow 1s^2 2l3l'[^{3,1}L_J]nl'', \end{aligned} \quad (3)$$

which again can radiatively decay emitting a photon when any one of the $2l$, $3l'$ or nl'' electrons drops into a lower subshell. Similarly values of l' up to $l' = 6$ were included along with values of n up to $n = 15$. Again an approximation for the high-level values of n was used up to $n = 1000$.

AUTOSTRUCTURE is implemented within the ADAS suite of programs as ADAS701. It produces raw autoionization and radiative rates which must be post-processed to obtain the final state level-resolved and total dielectronic recombination rates. A post-processor ADASDR is used to reorganize the resultant data and also to add in radiative transitions between highly-excited Rydberg states, which are computed hydrogenically. The ionic thresholds are shifted (by a small amount) to known spectroscopic values (typically taken from the NIST database) at this step. This post-processor outputs directly the *adf09* file necessary for use by ADAS. Separate files are produced for the different core excitations. For the beryllium isoelectronic sequence we calculate dielectronic recombination rate coefficients for the $\Delta n = 0$ and $\Delta n = 1$ transitions and so, generally, four *adf09* files are produced since we calculate in both the *LS* and intermediate-coupling configuration mixed approximations.

3. Results

The *adf09* files generated by our calculations in both the *LS* and intermediate-coupling configuration mixed approximations, for both the $\Delta n = 0$ and $\Delta n = 1$ transitions, are available on the www (`http://www-cfadc.phy.ornl.gov`). They provide final state level-resolved dielectronic recombination rate coefficients into final *LS* terms or *LS J* levels in a manner useful to fusion and astrophysical modellers. All of our total intermediate-coupling rate coefficients were also fitted with the following formula

$$\alpha = \frac{1}{T^{3/2}} \sum_{i=1}^{5} c_i e^{-E_i/T}, \quad (4)$$

to facilitate comparison with other work. In this equation T and E_i have units of Kelvin and the rate coefficients α have units cm^3/s. Our fits are accurate to better than 3%, for all ions in the temperature range $Z^2(5 \times 10^3 – 1 \times 10^7)$ K, where Z is the residual charge of the initial ion. In Table 1 we present a list of the coefficients c_i and E_i for each member of the beryllium isoelectronic sequence. In these fitting coefficients the contributions from the $\Delta n = 0$ and $\Delta n = 1$ transitions have been added together. We also plot some examples of the final state

Table 1. Fitting coefficients c_i and E_i for Eq. (5), for ions in the beryllium isoelectronic sequence. All coefficients refer to our intermediate-coupling calculations.

Ion	c1	c2	c3	c4	c5	E1	E2	E3	E4	E5
B^{+}	4.317(−5)	1.177(−3)	···	···	···	6.705(+4)	1.066(+5)	···	···	···
C^{2+}	9.146(−6)	5.045(−4)	3.742(−3)	···	···	6.485(+3)	1.052(+5)	1.458(+5)	···	···
N^{3+}	5.943(−5)	6.386(−4)	7.050(−3)	1.711(−5)	···	9.140(+3)	1.027(+5)	1.928(+5)	2.824(+6)	···
O^{4+}	1.925(−5)	1.246(−4)	4.556(−4)	1.083(−2)	9.868(−4)	8.552(+2)	1.640(+4)	6.560(+4)	2.229(+5)	8.160(+5)
F^{5+}	1.856(−4)	6.807(−4)	1.445(−2)	3.084(−3)	···	1.369(+4)	5.259(+4)	2.547(+5)	9.661(+5)	···
Ne^{6+}	2.388(−4)	9.831(−4)	1.385(−2)	6.672(−3)	5.548(−3)	2.190(+3)	5.207(+4)	2.473(+5)	5.026(+5)	1.435(+6)
Na^{7+}	3.676(−4)	1.840(−3)	1.778(−2)	6.817(−3)	1.196(−2)	1.473(+4)	4.533(+4)	2.875(+5)	5.525(+5)	1.711(+6)
Mg^{8+}	5.488(−5)	2.664(−3)	2.500(−2)	6.169(−3)	2.202(−2)	2.969(+3)	7.940(+4)	3.421(+5)	1.014(+6)	2.130(+6)
Al^{9+}	7.731(−4)	4.602(−3)	2.971(−2)	1.547(−2)	2.479(−2)	2.593(+4)	9.519(+4)	3.953(+5)	1.740(+6)	2.692(+6)
Si^{10+}	9.360(−4)	3.831(−3)	1.433(−2)	2.765(−2)	5.822(−2)	7.601(+3)	4.385(+4)	2.510(+5)	5.812(+5)	2.856(+6)
P^{11+}	1.419(−3)	3.063(−3)	2.559(−2)	2.355(−2)	8.595(−2)	1.005(+4)	6.061(+4)	3.209(+5)	7.609(+5)	3.302(+6)
S^{12+}	9.035(−4)	6.703(−3)	3.667(−2)	1.973(−2)	1.111(−1)	1.016(+4)	8.917(+4)	4.048(+5)	1.100(+6)	3.823(+6)
Cl^{13+}	7.505(−4)	8.945(−3)	3.737(−2)	2.663(−2)	1.455(−1)	7.187(+3)	6.959(+4)	4.024(+5)	1.078(+6)	4.320(+6)
Ar^{14+}	4.404(−3)	8.517(−3)	5.163(−2)	3.319(−2)	1.696(−1)	1.410(+4)	8.884(+4)	4.880(+5)	2.048(+6)	5.053(+6)
Ca^{16+}	5.330(−3)	2.413(−2)	6.421(−2)	2.556(−1)	4.604(−2)	2.952(+4)	2.192(+5)	7.855(+5)	5.472(+6)	8.821(+6)
Ti^{18+}	1.038(−2)	3.627(−2)	7.324(−2)	3.829(−1)	3.437(−1)	3.926(+4)	2.874(+5)	1.002(+6)	6.832(+6)	1.245(+7)
Cr^{20+}	5.166(−3)	2.729(−2)	9.046(−2)	1.534(−1)	4.407(−1)	4.068(+4)	2.073(+5)	8.092(+5)	5.012(+6)	9.748(+6)
Fe^{22+}	1.320(−2)	7.676(−2)	9.578(−2)	6.791(−1)	3.194(−2)	5.706(+4)	4.427(+5)	1.745(+6)	9.817(+6)	2.362(+7)
Ni^{24+}	2.848(−2)	1.093(−1)	1.146(−1)	8.347(−1)	3.499(−3)	9.194(+4)	6.413(+5)	2.848(+6)	1.194(+7)	2.444(+8)
Zn^{26+}	2.334(−2)	4.309(−2)	1.446(−1)	2.033(−1)	8.831(−1)	2.169(+4)	2.278(+5)	1.048(+6)	6.195(+6)	1.457(+7)
Kr^{32+}	9.331(−3)	9.982(−2)	2.376(−1)	3.905(−1)	1.251(+0)	1.646(+4)	3.813(+5)	1.677(+6)	9.924(+6)	2.118(+7)
Mo^{38+}	7.385(−2)	1.072(−1)	3.381(−1)	4.295(−1)	1.781(+0)	7.616(+4)	4.482(+5)	1.908(+6)	9.550(+6)	2.749(+7)
Xe^{50+}	1.826(−1)	1.918(−1)	6.962(−1)	9.599(−1)	2.047(+0)	5.853(+4)	8.194(+5)	3.766(+6)	1.847(+7)	4.880(+7)

level-resolved and total rate coefficients that are derived from the *adf09* files for several atomic ions in the beryllium-like sequence.

As an example of the final state level-resolved rate coefficients available, we present in Fig. 1 final state level-resolved dielectronic recombination rate coefficients for C^{2+}, calculated within the intermediate-coupling approximation described previously. The rate coefficients are from the initial $1s^22s^2\ ^1S_0$ level to the final state levels $1s^22s^22p\ ^2P_{1/2,3/2}$ and $1s^22s2p^2\ ^4P_{1/2,3/2,5/2}$ as indicated. Of course there exists hundreds of final state levels for this ion alone, for which the dielectronic recombination final state level-resolved rate coefficients are tabulated in the *adf09* files; here we plot several examples to illustrate the data. As expected, at low temperatures, the ion combines preferentially into the $1s^22s^22p\ ^2P_{1/2}$ level due to its lower energy. Some interesting structure is also observed in the rate coefficients for some of the other final state levels.

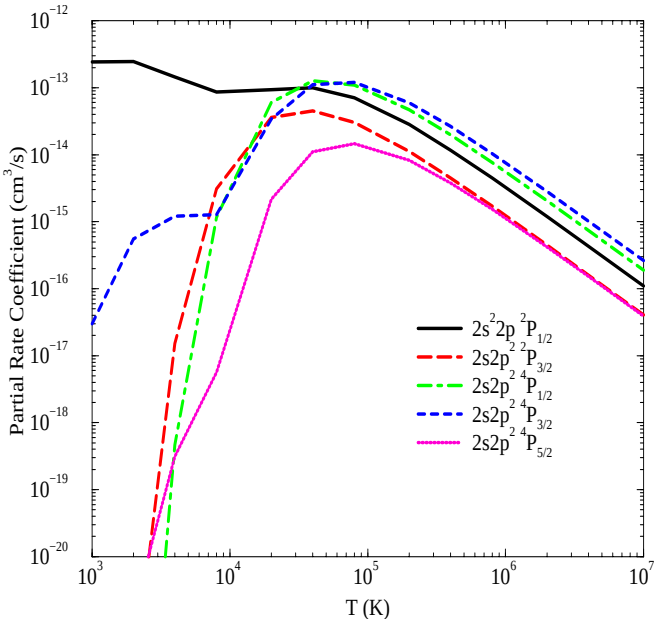

Fig. 1. Dielectronic recombination final state level-resolved rate coefficient for C^{2+} as a function of electron temperature (in Kelvin). We present final state level-resolved rate coefficients from the initial $1s^22s^2\ ^1S_0$ level to the final state levels as indicated (where we have dropped the $1s^2$ part of the configuration for clarity).

In Fig. 2 we present total dielectronic recombination rate coefficients for O^{4+}. We compare our *LS* and intermediate-coupling date with results fitted from the tables of Mazzotta et al. (1998), where they fitted to the calculations of Badnell & Pindzola (1989). We also show the calculations of Badnell & Pindzola (1989) in our figure. For high temperatures our results are in excellent agreement with the fitted coefficients of Mazzotta et al. (1998). However at low temperature (below 10^5 K) both our *LS* and intermediate-coupling results are significantly higher than the fit of Mazzotta et al. We also have plotted the data of Badnell & Pindzola (1989) to which the fit of Mazzotta et al. was made. It is clear that the results of Badnell & Pindzola (1989) are much closer to our results (especially the intermediate-coupling calculations) than to the fit of Mazzotta et al., suggesting that their fits become inaccurate at low temperatures.

To further illustrate our method and results, in Fig. 3 we present total rate coefficients for the dielectronic recombination

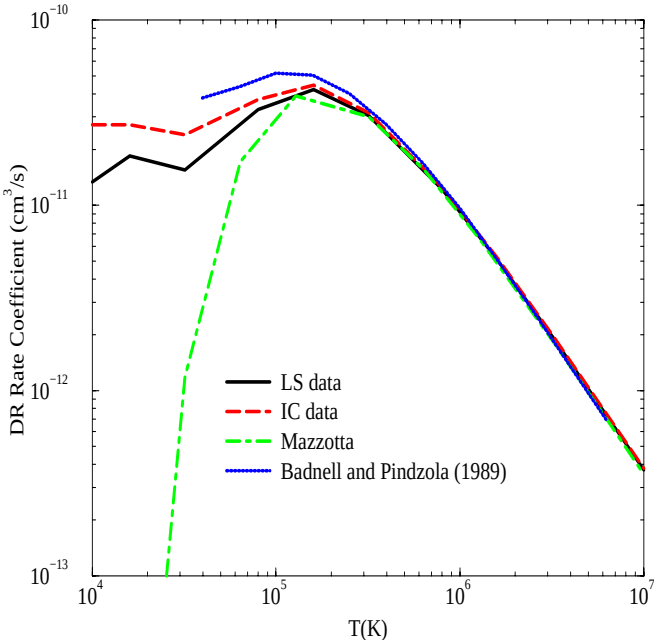

Fig. 2. Dielectronic recombination rate coefficient for O^{4+} as a function of electron temperature (in Kelvin). We compare our calculations using *LS* configuration mixing and intermediate-coupling configuration mixing with data from the fitted coefficients of Mazzotta et al., and with the calculations of Badnell & Pindzola.

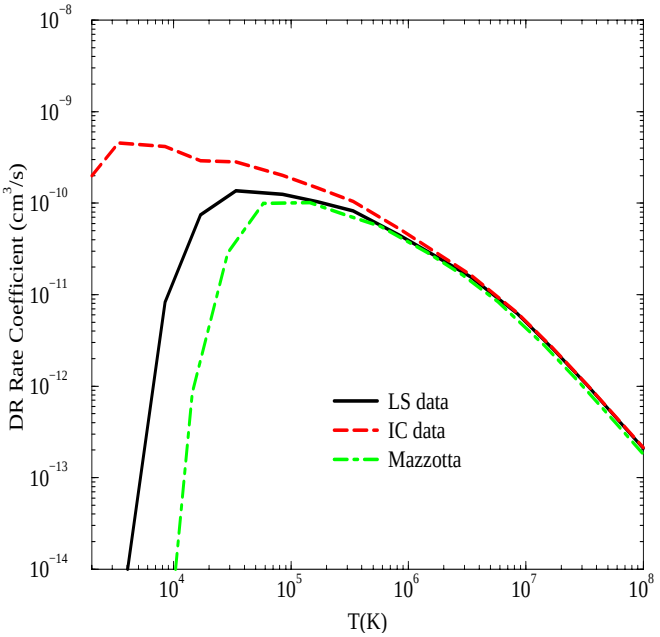

Fig. 3. Dielectronic recombination rate coefficient for Cl^{13+} as a function of electron temperature (in Kelvin). We compare our *LS* and intermediate-coupling calculations with the fitted coefficients of Mazzotta et al.

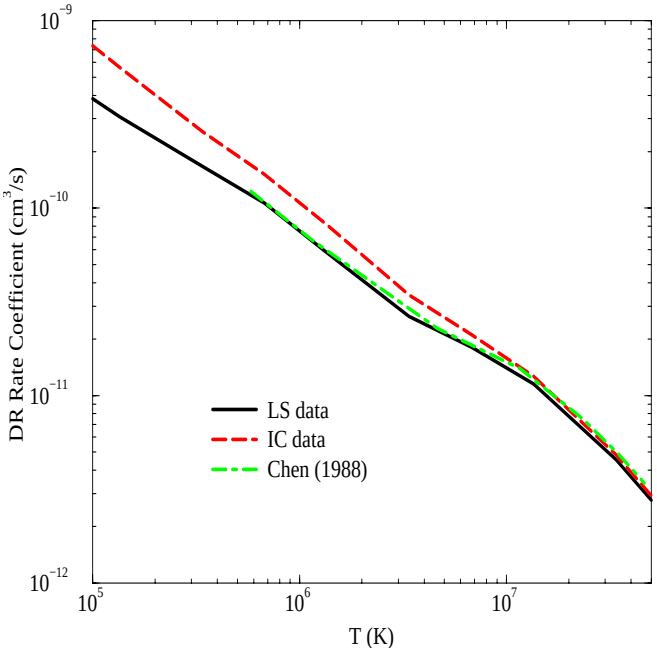

Fig. 4. Dielectronic recombination rate coefficient for Zn^{26+} as a function of electron temperature (in Kelvin). The *LS* and intermediate-coupling data are compared with data from Chen & Crasemann (1988).

of Cl^{13+}. In this case we again compare with the fitted coefficients of Mazzotta et al. (1989). For this ion, these fits were made to the calculations of Badnell (1987). Again at higher temperatures both sets of calculations are in good agreement with the fit of Mazzotta et al. At low temperature our *LS* calculations fall off sharply as do the fitted results. This is unlike the intermediate-coupling calculations which are much higher at the low temperatures.

Finally, in Fig. 4 we present total dielectronic recombination rate coefficients for Zn^{26+}. In this case we compare with data from Chen & Crasemann (1988), who used relativistic wave functions to study higher Z beryllium-like ions. Very good agreement is observed between our *LS* and intermediate-coupling calculations and the data of Chen & Crasemann, especially at high temperatures. In the lower temperature region, our intermediate-coupling calculations are slightly higher than both the *LS* calculations and those of Chen & Crasemann, which remain in excellent agreement.

4. Summary

In this paper we have described calculations of dielectronic recombination data for the beryllium-like isoelectronic sequence as part of an assembly of a dielectronic recombination database necessary for the modelling of dynamic finite-density plasmas (Badnell et al. 2003). We have calculated *LS J* final state level-resolved dielectronic recombination rate coefficients in a form which will prove of great use to astrophysical and fusion plasma modellers. Although our approximations are such that each final state level-resolved dielectronic recombination rate coefficient may not be as highly accurate as some of the most sophisticated techniques available today, we have calculated our data over a wide temperature range and for a large number of atomic ions in order to maximise the available information for modelling work.

We have presented selected final state level-resolved and total rate coefficients for some ions of interest and have

made comparisons, where possible, with previous work. In the high temperature range we have found good agreement with the calculations of Badnell (1987), which have been fitted by Mazzotta et al. (1998). However, it appears that the fits of Mazzotta et al. (1998) may become inaccurate in the low temperature range. We also comment that, at the lowest temperatures considered there may be a significant uncertainty in the dielectronic recombination rate coefficient due to an uncertainty in the position of near threshold resonances. However, these temperatures are likely to be too low to be of concern to plasma modelling, even for the case of photoionized plasmas. Our fits are accurate to better than 3%, for all ions in the temperature range $Z^2(5 \times 10^3$–$1 \times 10^7)$ K, where Z is the residual charge of the initial ion. In the future we will present dielectronic recombination data for further isoelectronic sequences as detailed previously (Badnell et al. 2003).

Note added in proof: After submission of the present article, a related study of DR rate coefficients appeared (Gu 2003) – preliminary comparisons show excellent agreement for the total rate coefficients.

Acknowledgements. This work was supported in part by the US Department of Energy. Computational work was carried out at the National Energy Research Scientific Computing Center in Oakland, CA.

References

Badnell, N. R. 1986, J. Phys. B, 19, 3827
Badnell, N. R. 1987, J. Phys. B, 20, 2081
Badnell, N. R. 1997, J. Phys. B, 30, 1
Badnell, N. R., O'Mullane, M., Summers, H. P., et al. 2003, A&A, 406, 1151
Badnell, N. R., & Pindzola, M. S. 1989, Phys. Rev. A, 39, 1690
Badnell, N. R., Pindzola, M. S., Andersen, L. H., Bolko, J., & Schmidt, H. T. 1991, J. Phys. B, 24, 4441
Chen, M. H., & Crasemann, B. 1988, Phys. Rev. A, 38, 5595
Dittner, P. F., Datz, S., Krause, H. F., et al. 1987, Phys. Rev. A, 36, 33
Gu, M. F. 2003, ApJ, 590, 1131
Mazzotta, P., Mazzitelli, G., Colafrancesco, S., & Vittorio, N. 1998, A&AS, 133, 403
Mitnik, D. M., Pindzola, M. S., & Badnell, N. R. 1999, Phys. Rev. A, 59, 3592
Pindzola, M. S., & Badnell, N. R. 1992, Nucl. Fusion and Plasma Material Interaction data for fusion, 3, 101
Pindzola, M. S., Badnell, N. R., & Griffin, D. C. 1992, Phys. Rev. A, 46, 5725
Summers, H. P. 2001, ADAS User Manual (2nd ed.), available from `http://adas.phys.strath.ac.uk/adas/docs/ manual`
Zatsarinny, O., Gorczyca, T. W., Korista, K. T., Badnell, N. R., & Savin, D. W. 2003, A&A, 412, 587